

PHYSICOCHEMICAL, ANTIOXIDANT AND CORROSION INHIBITION PROPERTIES OF *RHUS CORIARIA* L. EXTRACTS OBTAINED USING SOLVENTS OF DIFFERENT POLARITY

Gülşah GÖKCE^{1*}, Bahar TAN ÖZAY², Büşra ERDEM¹, Yakup ŞİRİN¹,
Perihan GÜRKAN¹, Nurdane YILMAZ³

¹Sem-As Food, Tourism, Industry and Trade Limited Company, Research and Development Unit, Ankara, Türkiye

²Kastamonu University Graduate School of Natural and Applied Sciences, Department of Materials Science and Engineering, Materials Science and Engineering, Kastamonu, Türkiye

³Kastamonu University Faculty of Education, Department of Mathematics and Science Education, Division of Science Education, Kastamonu, Türkiye

Received / Geliş: 03.11.2025; Accepted / Kabul: 27.01.2026; Published online / Online baskı: 31.03.2026

ABSTRACT

While the antioxidant properties of *Rhus coriaria* L. have been extensively documented, its systematic evaluation as a green corrosion inhibitor through a direct comparison between powder and seed forms has not been previously investigated. This study addresses this gap by examining the inhibition efficacy of sumac powder and seeds for mild steel in 1M HCl, where biomass forms are compared directly in their native states. To elucidate the underlying mechanism, a comprehensive characterization was conducted using extracts obtained with water, ethanol, acetone, and chloroform to identify the influence of solvent polarity on the biomass matrix. Physicochemical analyses revealed that the seed form, particularly in ethanolic profiles, exhibits a higher total phenolic content (267.4 mg GAE/100 g) and superior redox-active profiles. Electrochemical evaluations via potentiodynamic polarization and EIS demonstrated that inhibition efficiency reaches a maximum of 60.79% for the seed form at 200 ppm. This performance is established as a direct consequence of the seed matrix's higher antioxidant capacity and stabilized profile, which facilitate a more resilient adsorptive film than the powder form. This study proves that sumac seeds, as a byproduct, offer a robust protective layer through synergistic phytochemical interactions.

Keywords: Adsorption, antioxidants, corrosion, extraction, *Rhus coriaria* L.

FARKLI POLARİTEDEKİ ÇÖZÜCÜLERLE ELDE EDİLEN *RHUS CORIARIA* L. EKSTRAKTLARININ FİZİKOKİMYASAL, ANTİOKSİDAN VE KOROZYON İNHİBİSYONU

ÖZ

ÖZELLİKLERİ

Sumak (*Rhus coriaria* L.)'nin antioksidan özellikleri yaygın olarak belgelenmiş olsa da toz ve çekirdek formları arasındaki doğrudan bir karşılaştırma yoluyla yeşil korozyon inhibitörü olarak sistematik değerlendirmesi daha önce araştırılmamıştır. Bu çalışma, sumak tozu ve çekirdeklerinin 1M HCl ortamındaki korozyon inhibisyon etkinliğini, biyokütle formlarının doğrudan kıyaslandığı özgün bir kurguyla incelemektedir. Çözücü polaritesinin (su, etanol, aseton ve kloroform) biyokütle matrisi üzerindeki etkisini belirlemek ve mekanizmayı aydınlatmak amacıyla kapsamlı bir karakterizasyon yürütülmüştür. Fizikokimyasal analizler, çekirdek formunun toz formuna kıyasla daha yüksek toplam fenolik içeriği (267.4 mg GAE/100 g) ve üstün redoks-aktif profil sergilediğini göstermiştir. Elektrokimyasal değerlendirmeler, inhibisyon veriminin 200 ppm'de çekirdek formu için %60.79'a ulaştığını kanıtlamıştır. Elde edilen bu performansın, çekirdek formunun toz formuna kıyasla sahip olduğu üstün antioksidan kapasitesinin ve stabilize profilinin doğrudan bir sonucu olduğu ve metal yüzeyinde daha dirençli bir adsorpsiyon filmi oluşturduğu saptanmıştır. Bu çalışma, sumak çekirdeklerinin bir yan ürün olarak, sinerjik fitokimyasal etkileşimler yoluyla sağlam bir koruyucu şelat tabakası sağladığını kanıtlamaktadır.

Anahtar kelimeler: Adsorpsiyon, antioksidan, ekstraksiyon, korozyon, *Rhus coriaria* L.

INTRODUCTION

Rhus coriaria L., commonly known as sumac, is a perennial shrub belonging to the Anacardiaceae family, naturally distributed across the Mediterranean and Middle Eastern regions. The species is recognized in both traditional medicine and modern pharmacology for its red fruit clusters that ripen in autumn, characterized by their pronounced acidity. Throughout history, sumac has been valued for its antiseptic, digestive, and antipyretic properties, currently, it maintains a broad industrial application as a natural colorant, food preservative, and bioactive supplement. Recent investigations into the phytochemical profile of *Rhus coriaria* reveal that its phenolic constituents play a critical role in maintaining metabolic balance by mitigating oxidative stress (Al Quraishy et al., 2022). This bioactive capacity extends beyond cardiovascular protection, as its utilization in dermo-cosmetic formulations for wound healing and in oral hygiene products as an anti-pathogenic agent has also been reported (Yılmaz & Karakus, 2021).

The extraction process is recognized as the most critical stage in determining the biological activity of plant-derived bioactive compounds. Extraction efficiency is influenced by parameters such as temperature, duration, and methodology, with solvent polarity serving as the most decisive factor. While high-polarity solvents, such as water and ethanol, are effective in recovering hydrophilic phenolic acids and flavonoids, low-polarity solvents, including acetone and chloroform, are identified as more efficient for the extraction of lipophilic components such as fatty acids, terpenes, and sterols (Azmir et al., 2013). Recent studies emphasize that the selection of these solvents governs not only the extraction yield but also the capacity of the resulting phytochemicals to form protective layers on metallic surfaces and inhibit oxidative stress (Al-Amiery et al., 2023; Zannou & Koca, 2022).

The rich polyphenolic content of sumac provides a potent antioxidant capacity while positioning it as an effective candidate for "green corrosion inhibition" on metallic surfaces. A fundamental technical challenge in the food industry is the corrosion of stainless-steel processing equipment during acidic Cleaning-in-Place (CIP) procedures. Aggressive solutions, such as 1M HCl used for mineral scale removal, lead to equipment degradation and significant food safety risks. The toxicity risks associated with synthetic inhibitors on food contact surfaces have increased the demand for natural alternatives like sumac.

Contemporary research confirms that sumac extracts can effectively inhibit metallic dissolution by forming a protective film through adsorption on steel surfaces (Bedair et al., 2022; Gökçe & Coşkuner, 2023).

Although numerous studies have documented the antioxidant properties of *Rhus coriaria*, a systematic comparative evaluation of the electrochemical corrosion inhibition performance of its different physical forms, seed and powder in relation to solvent polarity represents a significant gap in the literature. The variations between the protective lipid matrix of the seed tissue and the high practical applicability of the powder form, and how these factors influence the stability of the anti-corrosive film, have not yet been fully elucidated. In this context, the present study aims to determine the physicochemical properties of extracts obtained from sumac seed and powder forms using solvents of varying polarities and to comparatively evaluate the corrosion inhibition potentials of these forms in a 1M HCl environment.

MATERIALS AND METHODS

Material

The *Rhus coriaria* L. fruits used in this study were collected from the Konak district of İzmir, Türkiye. The seed samples were ground using a laboratory-scale ball mill (Testform, Türkiye) to obtain a uniform particle size for experimental analyses. To prepare the powdered form, a vibrating sieve system (Utest, Türkiye) was employed to achieve the desired granulation and homogeneity. The samples were sieved to a consistent particle size of less than 500 µm (35 mesh) to maximize the surface area to solvent ratio and ensure uniform mass transfer during the extraction process. This standardized particle size was maintained across all samples to eliminate physical variability prior to chemical and electrochemical evaluations.

Method

Extraction of sumac seed and powder samples was carried out using four different solvents, water, ethanol, acetone, and chloroform. In each procedure, 50 g of powdered or whole seed material was combined with 200 mL of the corresponding solvent. The mixtures were incubated in a shaking apparatus (Phoenix Instruments, Netherlands) operating at 200 rpm for 24 hours under ambient temperature conditions. After the extraction period, the suspensions were passed through

Whatman No. 1 filter paper to separate the solid residues. The resulting filtrates were collected and stored in sealed containers at 4 °C until subsequent physicochemical and analytical analyses were conducted.

Physicochemical analysis

Ph value

The pH of the extracts was analyzed following the procedures outlined in TS 1728 and ISO 1842 standards, employing a calibrated pH meter (Hanna Instruments, HI 2020, USA). Measurements were carried out at a controlled temperature of 20 °C to maintain precision and consistency. Each extract was analyzed three times, and the average value was reported. This approach provided a dependable assessment of the acidic–basic properties of the extracts and allowed the comparison of solvent-related differences in extraction performance.

Determination of electrical conductivity

Electrical conductivity of the extracts was determined by a conductivity meter (Ohaus, ST300C, USA) operated under standard laboratory conditions. Measurements were performed at a controlled temperature of 20 °C to ensure precision and reproducibility. Each extract was tested three times, and the average results were recorded. Subsequently, the influence of solvent type on the electrical conductivity of the extracts was analyzed and compared.

Determination of total soluble solids (°Brix)

The total soluble solids of the extracts were quantified using a benchtop refractometer (Abbe-2, Ertich, Germany). Results were reported as degrees Brix (°Brix), indicating the relative concentration of dissolved solids within each extract. All measurements were performed at a controlled temperature of 20°C, and triplicate readings were obtained to ensure consistency and analytical reliability.

Colour measurement (Hunter colour analysis)

Colour properties of the samples were analysed using a colorimeter (Konica Minolta, CR-410, Japan). Measurements were conducted based on the CIE L*, a*, and b* colour space coordinates. Within this model, the L* value indicates brightness (ranging from 0 for black to 100 for white), the a* coordinate describes the red–green spectrum (positive values denote red, negative values denote green), while the b* coordinate corresponds to the yellow–blue axis (positive for yellow and negative for blue).

Each sample was measured three times independently, and average readings were used for evaluation. Before analysis, the device was standardized with a white reference plate to ensure measurement precision and repeatability.

Determination of ash content

The ash content of the samples was quantified through the gravimetric procedure outlined by the Association of Official Analytical Chemists (AOAC, 2000). All weighing were performed using a high-precision analytical balance (RADWAG, AS220. R2, Poland). Approximately 2 g of each sample was precisely measured (± 0.01 mg) and placed into pre-dried, pre-weighed porcelain crucibles. The material was initially carbonized over a Bunsen burner and then subjected to complete incineration in a muffle furnace at 550 °C until a stable mass and a pale grey to white ash appearance were achieved.

The remaining residue was weighed, and the ash percentage was computed relative to the initial mass of the sample. To maintain analytical accuracy and repeatability, each determination was conducted in triplicate.

Determination of protein content

The protein concentration of the extracts was analyzed using the Kjeldahl procedure in accordance with the AOAC (2000) guidelines. Approximately 1 g of each dried sample was digested with concentrated sulfuric acid (H_2SO_4) in the presence of a mixed catalyst until complete mineralization and a clear solution were achieved. The digests were subsequently distilled, during which the liberated ammonia was absorbed in a boric acid solution and then titrated with standardized hydrochloric acid (HCl).

Total nitrogen was determined and converted to crude protein content by applying a conversion coefficient of 6.25. All determinations were performed in triplicate to ensure analytical reliability and reproducibility.

Determination of antioxidant activity

FRAP analyses (Ferric reducing antioxidant power)

The antioxidant capacity was determined using the Ferric Reducing Antioxidant Power (FRAP) assay according to the procedure established by Benzie and Strain (1996). The reduction of the Fe(III)–TPTZ complex was monitored at 593 nm using a UV–VIS spectrophotometer (SHIMADZU, UV-1900I, Japan). Results were quantified using a $\text{FeSO}_4 \cdot 7\text{H}_2\text{O}$

calibration curve (31.25–1000 μM) and expressed as μM $\text{FeSO}_4 \cdot 7\text{H}_2\text{O}$ equivalents. The specific reagent compositions and

detailed pipetting protocols are provided in the Supplementary Material (Table S1 and Figure S1).

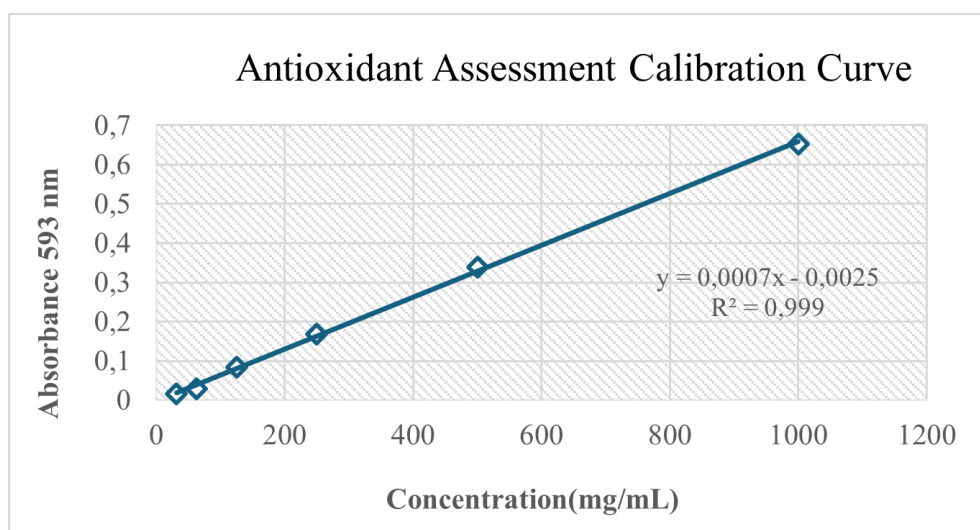


Figure S1. Antioxidant assessment calibration curve

Table S1. Pipetting procedure in FRAP determination

	Blank _{MeOH}	Test (Sample)	Color Blank _{MeOH}	$\text{FeSO}_4 \cdot 7\text{H}_2\text{O}$
FRAP Reagent	3 mL	3 mL	-	3 mL
Sample (Sumac extracts)	-	100 μL	100 μL	-
$\text{FeSO}_4 \cdot 7\text{H}_2\text{O}$ (Variable Conc.)	-	-	-	100 μL
Methanol	100 μL	-	3 mL	-

*In the 4th minute, absorbance is read at 593 nm.

*Colour Blank MeOH: Colour blank for the sample dissolved in methanol

DPPH free radical scavenging activity analysis

The free radical scavenging activity of the extracts was evaluated using the DPPH• (2,2-diphenyl-1-picrylhydrazyl) assay, based on the analytical principles described by Cuendet et al. (1997). The reduction of the stable DPPH radical by antioxidant molecules was monitored spectrophotometrically by the

decrease in absorbance at 517 nm. The antioxidant efficiency was quantified as the SC_{50} value (mg/mL), representing the concentration required to inhibit 50% of the DPPH radicals, derived from dose-response curves. The comprehensive pipetting sequence and procedural details are provided in the Supplementary Material (Table S2).

Table S2. Pipetting procedure in DPPH determination

	Blank	Color Blank	Sample
Sample (Sumac extracts)	-	750 μL	750 μL
Methanol	750 μL	750 μL	-
DPPH•	750 μL	-	750 μL

*In the 4th minute, absorbance is read at 593 nm.

*Colour Blank MeOH: Colour blank for the sample dissolved in methanol

Total phenolic content analysis

The Total Phenolic Content (IPC) of the extracts was determined using the Folin-Ciocalteu colorimetric assay, as described by Slinkard and Singleton (1977). The method involves the reduction of the Folin-Ciocalteu reagent by phenolic compounds under alkaline conditions, with the resulting blue-violet complex measured spectrophotometrically

at 760 nm (SHIMADZU, UV-1900I, Japan). Phenolic concentrations were quantified through a gallic acid calibration curve (1.000–0.015625 mg/mL) and expressed as milligrams of gallic acid equivalents (mg GAE). The specific calibration curve and detailed pipetting layout are provided in the Supplementary Material (Table S3 and Figure S2, respectively).

Table S3. Pipetting procedure for total polyphenolic determination

	Blank	Color Blank	Standard	Sample
Sample	-	250 μ L	-	250 μ L
Standard (Quercetine)	-	-	250 μ L	-
Methanol	2.4 mL	2.25 mL	2.15 mL	2.15 mL
1M $\text{NH}_4\text{CH}_3\text{COO}$	50 μ L	-	50 μ L	50 μ L
10% $\text{Al}(\text{NO}_3)_3$	50 μ L	-	50 μ L	50 μ L

*In the 4th minute, absorbance is read at 415 nm.

*Color Blank MeOH: Color blank for the sample dissolved in methanol.

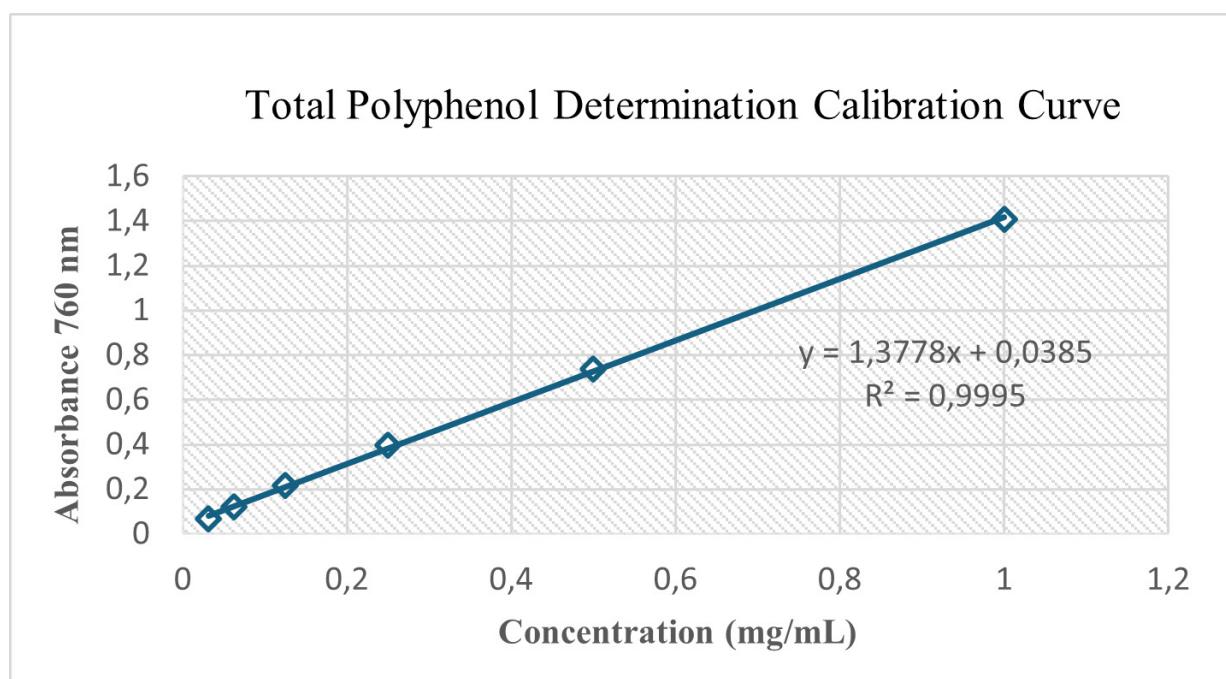


Figure S2. Total polyphenol determination calibration curve

Electrochemical corrosion resistance analysis

The corrosion inhibition performance of sumac extracts was evaluated on C20 mild steel in a 1M HCl environment using a Gamry Reference 3000 Potentiostat/ Galvanostat (Gamry Instruments, USA). A standard three-electrode cell was utilized, consisting of a mild steel working electrode (exposed area: 0.3846 cm²), an Ag/AgCl reference electrode and a graphite counter electrode. Prior to measurements, the electrode surface was polished with SiC papers up to 1200 grit, rinsed and immersed in the medium for 30 minutes to reach the Open Circuit Potential (OCP).

Electrochemical Impedance Spectroscopy (EIS) was performed at OCP within a frequency range of 105 Hz to 0.2 Hz using a 10 mV sinusoidal perturbation. The inhibition efficiency ($\% \eta_{EIS}$) was calculated from the polarization resistance (R_p) values using Equation (1) (Verma et al., 2018).

$$\% \eta_{EIS} = \left[1 - \frac{R_{p,o}}{R_{p,i}} \right] \times 100 \quad (\text{Equation 1})$$

Where $R_{p(inh)}$ and $R_{p(0)}$ denote the polarization resistance for the inhibited and uninhibited systems, respectively.

Potentiodynamic Polarization (Tafel) measurements were conducted within a range of ± 250 mV vs. OCP at a scan rate of 1 mV s⁻¹. The inhibition efficiency ($\%IE$) and surface coverage (θ) were determined using Equations (2) and (3) (Fouda & Abdel-Gaber, 2020).

$$\%IE = \left[1 - \frac{I_{corr}^*}{I_{corr}} \right] \times 100 \quad (\text{Equation 2})$$

$$\theta = \left[1 - \frac{I_{corr}^*}{I_{corr}} \right] \quad (\text{Equation 3})$$

Where I_{corr}^* and I_{corr} are the corrosion current densities measured in the absence and presence of the inhibitor, respectively.

RESULT and DISCUSSION

pH profiles of extracts obtained from sumac (*Rhus coriaria* L.) powder and seeds in different solvent systems

The pH values of the extracts obtained from sumac powder and seeds displayed significant variations depending on the solvent type and the physical form of the biomass ($P < 0.05$). As presented in Table 1., the pH values ranged from 2.84 ± 0.03 to 3.67 ± 0.05 . The statistical analysis using Tukey's HSD test revealed that each experimental group belonged to a distinct statistical subset (indicated by letters a-d), confirming that the interaction between solvent polarity and particle size is a critical determinant of the final chemical environment.

Table 1. pH values of sumac powder and sumac seed extracts (mean \pm SD)

Sample Form	Water	Ethanol	Acetone	Chloroform
Sumac powder	3.09 ± 0.01^b	2.84 ± 0.03^d	N.D.	N.D.
Sumac seed	2.93 ± 0.02^c	3.67 ± 0.05^a	N.D.	N.D.

N.D.: Not detected.

The aqueous extracts of both powder and seed forms exhibited a highly acidic profile, with pH values of 3.09 ± 0.01 and 2.93 ± 0.02 , respectively. This inherent acidity is attributed to the efficient leaching of indigenous organic acids predominantly malic, citric, and tartaric acids into the polar aqueous medium. These results are in strong agreement with the findings of Bursal and Köksal (2011), who reported similar acidity levels for Mediterranean sumac genotypes. The lower pH observed

in the aqueous seed extract compared to the powder suggests a higher localized concentration of soluble acids within the seed matrix, which is effectively mobilized by water (Kossah et al., 2009).

In the case of ethanolic extracts, a more pronounced divergence was observed. The powder form in ethanol yielded the most acidic profile of the entire study (2.84 ± 0.03 , Tukey 'd'). This

can be scientifically explained by the increased surface area of the pulverized powder, which facilitates the rapid release of acidic phenolic compounds and tannins into the ethanol, a solvent known for its high efficiency in recovering bioactive fractions (Uysal & Zengin, 2021). Conversely, the ethanolic seed extract showed the highest pH value (3.67 ± 0.05 , Tukey 'a'). This "neutralizing" trend likely results from the lower solubility of polar organic acids in ethanol when compared to water, coupled with the potential buffering effect of the lipid-rich matrix found in the sumac seed (Abu Reidah et al., 2015). The absence of pH measurements (N.D.) for acetone and chloroform extracts is consistent with the aprotic nature of these solvents. Since the pH scale is fundamentally defined by the concentration of hydronium ions (H_3O^+) in protic systems, measurements in non-polar, aprotic media are methodologically invalid (Holler & Crouch, 2018). From a corrosion science perspective, the acidic nature of the aqueous and ethanolic extracts is highly beneficial. Such low pH environments

facilitate the protonation of functional groups in the inhibitor molecules, thereby promoting their adsorption onto the metal surface to form a protective barrier in acidic 1M HCl solutions (Nawaz et al., 2020).

Electrical Conductivity (EC) values of extracts obtained from sumac (*Rhus coriaria* L.) powder and seeds in different solvent systems

The electrical conductivity (EC) of the extracts was analyzed to evaluate the ionic solubility and mass transfer efficiency from the sumac matrix into various solvent systems. As shown in Table 2., the EC values exhibited significant variations ($P < 0.0001$), influenced by the synergistic effect of solvent polarity and the physical form of the biomass. The distinct Tukey HSD letters (a, b) within each solvent group confirm that the powder and seed forms are statistically differentiated in terms of their ion-releasing capacities.

Table 2. Electrical conductivity values of sumac powder and seed extracts ($\mu S/cm$, mean \pm SD)

Sample Form	Water	Ethanol	Acetone	Chloroform
Sumac powder	$16.5 \times 10^3 \pm 0.06^a$	843.00 ± 1.73^b	88.63 ± 1.15^a	N.D.
Sumac seed	$5.18 \times 10^3 \pm 0.345^b$	$50.87 \times 10^3 \pm 0.64^a$	42.53 ± 0.25^b	N.D.

N.D.: Not detected.

In the powder form, the highest conductivity was recorded in the aqueous extract ($16.5 \times 10^3 \mu S/cm$), whereas in the seed form, the maximum value was observed in the ethanolic extract ($50.87 \times 10^3 \mu S/cm$). These findings underscore the critical role of solvent dielectric constants in determining ionic mobility. According to Wang et al. (2023), high polarity solvents significantly enhance ion solubility in botanical matrices, while low polarity solvents, such as acetone and chloroform, severely restrict ion release due to limited solvation energy (Zhao et al., 2022). The not determined (N.D.) values in chloroform are consistent with its non-polar, aprotic nature, which prevents the stabilization of free ions.

The significant differences between the powder and seed forms are primarily attributed to the effective surface area and cellular integrity. The reduction in particle size in the powder form increases the contact area with the solvent, facilitating rapid ion leaching. This is supported by Li et al. (2021), who stated that

comminution significantly improves ionic solubility in plant extracts. Interestingly, the exceptionally high EC value of the seed form in ethanol ($50.87 \times 10^3 \mu S/cm$) suggests that ethanol may be more effective at penetrating the intact seed coat to mobilize specific ionic constituents compared to water.

In the context of this study, EC serves as a vital indicator of solvent-matrix interactions rather than a simple quality parameter. High EC values reflect a robust extraction of ionic species, which often correlates with the presence of protonated phenolic groups and organic acid salts. For corrosion inhibition applications, a higher ionic presence in the extract can influence the electrolyte's conductivity and the subsequent formation of the protective double layer on the metal surface (Almuhayawi, 2022).

Soluble solid content (°Brix) of sumac extracts

The °Brix values of *Rhus coriaria* extracts were evaluated to quantify the total soluble solids (TSS) as an indicator of

extraction yield. As shown in Table 3., the solubility profiles were significantly affected by the solvent's chemical nature ($P<0.05$). Chloroform extracts reached the highest TSS levels

(up to 62.17 ± 0.25), whereas aqueous extracts exhibited the lowest values, highlighting a strong correlation between solvent dielectric constants and the mass transfer of sumac metabolites.

Table 3. °Brix measurement results of sumac powder and seed extracts (mean±standard deviation)

Sample form	Water	Ethanol	Acetone	Chloroform
Sumac powder	3.70 ± 0.00^d	21.90 ± 0.10^b	20.50 ± 0.10^c	62.17 ± 0.25^a
Sumac seed	4.17 ± 0.06^d	23.60 ± 0.26^b	22.27 ± 0.15^c	60.80 ± 0.30^a

The exceptionally high °Brix values in chloroform are consistent with the findings of Doğan and Çelik (2012), who reported that non-polar solvents are highly effective in recovering the fixed oil and hydrophobic terpenoid fractions that constitute a major portion of the sumac drupe. Furthermore, the significant soluble solid content in ethanol (21.90-23.60) aligns with the work of Shamsudin et al. (2022), where ethanol was shown to have a superior capacity for simultaneous extraction of both polar and semi-polar compounds, such as anthocyanins and hydrolysable tannins.

The distinction between the powder and seed forms also played a vital role. The higher °Brix values observed in seed extracts across most solvents can be explained by the gradual release of concentrated solutes from the endocarp, a process often influenced by the internal osmotic pressure of the seed during prolonged extraction (Ghafoor et al., 2011). In contrast, the low values in water (3.70-4.17) suggest that while water is excellent for organic acids (as seen in pH results), it fails to solubilize the dominant lipophilic and resinous components of

the sumac fruit, a phenomenon documented in the solubility studies of Spigno et al. (2007).

Statistical analysis via Tukey's HSD confirmed that chloroform, ethanol, and water form three distinct efficiency tiers. This hierarchy demonstrates that maximizing the recovery of total dissolved solids from *Rhus coriaria* requires solvents with low to intermediate polarity, as high-polarity aqueous environments only target a small fraction of the available biomass (Mustafa & Turner, 2011).

CIELAB Colour Analysis and Pigment Composition

The colorimetric parameters (L^* , a^* , b^*) of the *Rhus coriaria* extracts were analyzed to determine the influence of solvent polarity and biomass form on the release of natural pigments. As presented in Table 4., significant variations in color space coordinates were observed ($P<0.05$). In the powder form, the L^* values ranged from 18.82 to 27.07, while a^* and b^* values varied between -0.32 to 12.39 and 0.64 to 4.54, respectively.

Table 4. Hunter colour parameters (L^* , a^* , b^*) of powdered and seed sumac extracts determined in different solvent media

Sample	L^*	a^*	b^*
Sumac powder Water	27.07	12.39	3.14
Sumac powder Ethanol	18.82	0.90	0.64
Sumac powder Acetone	19.69	1.10	1.58
Sumac powder Chloroform	23.80	-0.32	4.54
Sumac seed Water	20.5	2.19	0.95
Sumac seed Ethanol	21.33	0.99	2.36
Sumac seed Acetone	19.41	0.7	0.9
Sumac seed Chloroform	19.47	0.27	1.95

The aqueous powder extract exhibited the highest L* (lightness) and a* (redness) values (27.07 and 12.39, respectively). This distinct chromatic profile is attributed to the high solubility of anthocyanins and water-soluble phenolic pigments in polar media, facilitated by the increased surface area of the pulverized powder. These findings align with Mert et al. (2022), who reported that the release of red pigments in sumac is highly dependent on particle size reduction, which enhances the mass transfer of vacuolar pigments into the solvent.

The shift in color parameters is not merely a result of pigment concentration but is also influenced by the chemical environment, such as pH and ionic strength, which affect the structural stability of anthocyanins. The formation of colloidal phases and suspended micro-particles likely alters the light scattering properties of the extracts, contributing to the observed variations in L* and b* values (Salamat et al., 2023). Regarding solvent effects, high-polarity solvents like water promoted more vibrant red tones (higher a*), whereas acetone and ethanol yielded darker, less saturated extracts. Conversely, the chloroform extracts displayed significantly higher b*

(yellowness) values (up to 4.54), indicating a transition toward yellowish hues. This phenomenon is scientifically explained by the preferential solubilization of lipophilic pigments, such as carotenoids and xanthophylls, in non-polar media. According to Rodrigues et al. (2022), the yellowish chromatic shift in lipophilic sumac extracts is further influenced by the optical density and the specific light scattering behavior of the plant matrix when exposed to non-aqueous solvents. These results confirm that the colorimetric profile of *Rhus coriaria* extracts is a direct reflection of the solvent's selectivity for specific phytochemical classes.

Proximate Analysis: Ash and Protein Content of Sumac Extracts

The ash (%) and protein (mg/mL) contents of *Rhus coriaria* L. extracts were investigated to characterize the mineral and macromolecular distribution across different solvent systems. As presented in Table 5., both parameters were significantly influenced by the solvent type and the physical form of the biomass ($P < 0.05$).

Table 5. Ash (%) and protein (mg/ml) contents of powdered and seed sumac extracts in different solvent media

Sample Form	Ash (%)	Protein (mg/mL)
Sumac powder Water	0.8 ± 0.002^a	0.0037 ± 0.004^c
Sumac powder Ethanol	0.12 ± 0.005^c	0.437 ± 0.021^a
Sumac powder Acetone	0.07 ± 0.01^d	0.036 ± 0.003^b
Sumac powder Chloroform	0.1 ± 0.004^c	N.D.
Sumac seed Water	0.04 ± 0.02^c	0.028 ± 0.002^c
Sumac seed Ethanol	0.06 ± 0.004^d	0.420 ± 0.003^a
Sumac seed Acetone	0.06 ± 0.003^d	0.037 ± 0.003^b
Sumac seed Chloroform	0.09 ± 0.003^c	N.D.

N.D.: Not detected.

The highest ash content was observed in the aqueous powder extract ($0.8 \pm 0.002\%$), which was statistically classified into the highest group (Tukey 'a'). This elevated mineral recovery is attributed to the high solubility of inorganic ions such as potassium, calcium, and magnesium in polar aqueous media.

According to Galanakis (2021), inorganic components in plant matrices often exist in soluble fractions that preferentially migrate into the liquid phase during polar extraction. Furthermore, the reduction of particle size in the powder form facilitates the diffusion-controlled release of minerals by

weakening the ionic interactions between minerals and cell wall polysaccharides (Chemat et al., 2019).

In contrast, the seed extracts exhibited significantly lower ash contents (0.04–0.09%), falling into Tukey groups ‘d’ and ‘e’. This limited mineral recovery suggests that inorganic constituents in sumac seeds are predominantly sequestered within lignocellulosic structures or stabilized through complexes with phytates, which restrict their mobilization into the solvent (Sandberg, 2021). The non-polar chloroform extracts also showed minimal ash levels, confirming that the absence of co-extraction phenomena and limited solvent-matrix interaction prevent the transport of inorganic salts into aprotic media (Putnik et al., 2019).

Regarding protein content, the ethanolic extracts of both powder and seed forms yielded the highest concentrations (0.437 ± 0.021 mg/mL and 0.420 ± 0.003 mg/mL, respectively), forming a distinct statistical group (Tukey ‘a’). The superior efficiency of ethanol in protein recovery is likely due to its ability to weaken protein-matrix interactions and limit protein aggregation. Alamprese and Casiraghi (2022) stated that organic solvents can induce subtle conformational changes in protein structures, rendering hydrophobic regions more accessible and thereby increasing the soluble protein fraction.

The negligible difference in protein yield between the powder and seed forms in ethanol suggests that these proteins are primarily intracellular and can be effectively mobilized regardless of the degree of tissue fragmentation (Loveday, 2020). Conversely, the absence of detectable protein in chloroform and the low yields in water highlight the limitations of apolar and purely aqueous environments in stabilizing sumac proteins. In aqueous media, proteins may remain bound to the matrix or undergo reduced solubility due to complexation with other hydrophilic metabolites (Damodaran, 2017). These findings indicate that solvent selection is the primary determinant for the recovery of nitrogenous compounds from *Rhus coriaria*.

Antioxidant capacities (FRAP, DPPH) and total phenolic content (TPC)

The antioxidant potential and total phenolic concentrations of *Rhus coriaria* extracts were evaluated to determine the efficacy of different extraction strategies. As summarized in Table 6., the synergistic effect of solvent polarity and biomass form led to statistically significant variations across all measured parameters, including FRAP, DPPH, and TPC ($P < 0.05$ for each independent ANOVA model).

Table 6. Antioxidant capacity (FRAP and DPPH) and total phenolic content of sumac powder and seeds in different solvents

Sample Form	Antioxidant- FRAP (mg/ 100 g FeSO ₄)	Antioxidant- DPPH SC50 (mg/ mL)	Total phenolic (mg GAE/100 g)
Sumac powder Water	2.01 ± 0.15^f	0.93 ± 0.04^d	5.8 ± 0.5^f
Sumac powder Ethanol	26.92 ± 1.8^d	0.18 ± 0.01^a	32.4 ± 0.018^c
Sumac powder Acetone	115.32 ± 6.5^b	0.38 ± 0.02^b	156 ± 0.017^b
Sumac powder Chloroform	N.D.	0.44 ± 0.03^c	3.1 ± 0.2^f
Sumac seed Water	66.21 ± 3.2^c	0.72 ± 0.03^d	108 ± 1.4^c
Sumac seed Ethanol	198.82 ± 9.1^a	0.12 ± 0.01^a	267.4 ± 3.5^a
Sumac seed Acetone	21.18 ± 1.5^c	0.31 ± 0.02^b	41.3 ± 1.9^d
Sumac seed Chloroform	N.D.	0.42 ± 0.02^c	4.7 ± 0.3^f

N.D.: Not detected.

Ferric Reducing Antioxidant Power (FRAP) and Redox Dynamics

The FRAP assay results revealed that the antioxidant capacity of sumac varied significantly depending on both the sample form and the solvent used ($P < 0.05$). Specifically, the ethanolic seed extract was classified into the highest statistical group (Tukey 'a'), significantly outperforming all other treatments with a reducing power of 198.82 ± 9.1 mg/100 g FeSO_4 . Given that the FRAP method evaluates antioxidant capacity based on electron transfer-driven reducing power rather than radical scavenging, this finding highlights the decisive role of the redox potential of the extracted compounds. According to Apak et al. (2016), even samples with similar total phenolic contents can exhibit divergent FRAP responses depending on the structural features and electron donating capacities of the specific phenolic constituents. The superior performance of the seed form suggests a high concentration of redox-active flavanols and proanthocyanidins (Yüksel & Kaplan İnce, 2023).

DPPH Radical Scavenging Activity

The DPPH free radical scavenging results largely supported the trends observed in the FRAP analysis. The lowest SC₅₀ value (indicating the highest scavenging capacity) was recorded for the ethanolic seed extract (0.12 ± 0.01 mg/mL), placing it in the top statistical tier ($P < 0.05$). Generally, seed extracts exhibited lower SC₅₀ values (0.12–0.72 mg/mL) compared to powder extracts (0.18–0.93 mg/mL). Considering that the DPPH method operates via a hydrogen atom transfer mechanism, these results indicate that the compounds in the seed extracts possess a superior capacity for radical stabilization. These findings are consistent with Al Juhaimi et al. (2024), who reported high antioxidant activities for sumac fruit, emphasizing that the extraction strategy is a key determinant of biological performance.

Total Phenolic Content (TPC) and Phytochemical Synergy

The TPC analysis, based on the Folin-Ciocalteu reagent, provided a general indicator of the phenolic levels in the extracts. The values ranged from 3.1 to 267.4 mg GAE/100 g, with the maximum yield achieved in the ethanolic seed extract (267.4 ± 3.5 mg GAE/100 g, $P < 0.05$). However, since the Folin-Ciocalteu reagent can react with non-phenolic reducing compounds, TPC should be interpreted as a complementary parameter rather than a direct measure of functional antioxidant

activity. As noted by Alsamri et al. (2021), sumac extracts may exhibit different functional behaviors despite having similar total phenolic levels, as the biological efficacy depends on the specific structural classes present.

The high antioxidant activity in sumac seed extracts is likely driven by anthocyanins and hydrolysable tannins, such as pentagalloyl glucose and gallic acid derivatives. Koşar et al. (2006) reported that these specific fractions exhibit exceptionally low EC₅₀ values for the DPPH radical, confirming their potent scavenging capacity. From a corrosion science perspective, these high-TPC and redox-active extracts are ideal candidates for metal protection, as their numerous hydroxyl groups facilitate the formation of a stable, protective chelate layer on the steel surface in acidic 1M HCl environments.

Investigation of the corrosion inhibitory effects of sumac powder and seed on mild steel

The corrosion inhibition performance of *Rhus coriaria* powder and seed forms was evaluated using potentiodynamic polarization and electrochemical impedance spectroscopy (EIS) in a 1M HCl environment. The impact of these sumac forms on the anodic and cathodic polarization behavior of mild steel is illustrated in the Tafel plots. As shown in Figures 1. and 2., the addition of both powder and seed forms led to a prominent shift of the polarization curves toward lower current densities.

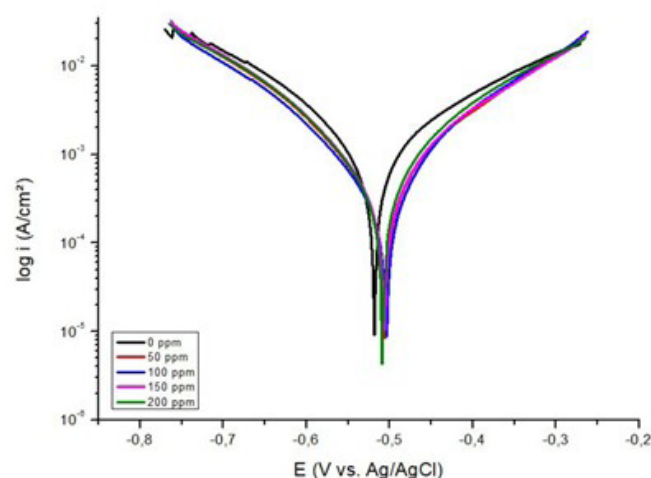


Figure 1. Tafel polarization curves of mild steel in 1M HCl containing different concentrations (50–200 ppm) of sumac powder extract.

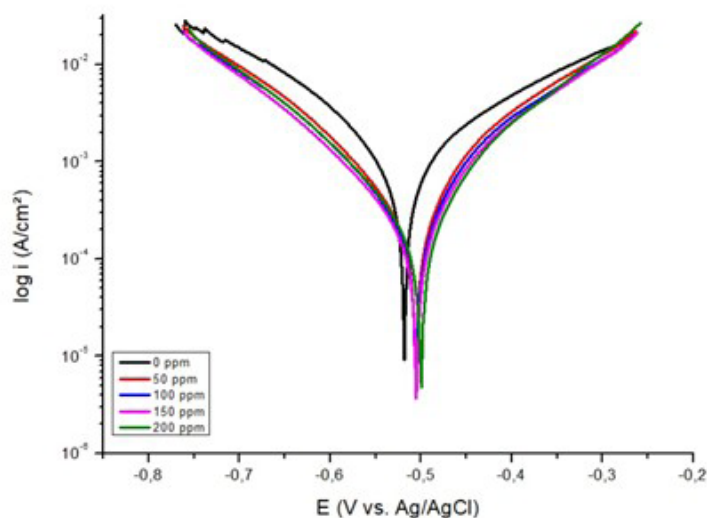


Figure 2. Tafel polarization curves of mild steel in 1M HCl containing different concentrations (50-200 ppm) of sumac seed extract.

Description: The decrease in current density and the shift in potential observed in the Tafel curves indicate the effectiveness of sumac seed extract as a corrosion inhibitor.

This observation is quantitatively supported by Tables 7. and 8., where the corrosion current density (I_{corr}) decreased from $\mu\text{A}/\text{cm}^2$ to $\mu\text{A}/\text{cm}^2$ for the powder and $\mu\text{A}/\text{cm}^2$ for the seed,

respectively, at 200 ppm. The maximum inhibition efficiency (%IE) was recorded as 60.79% for the seed form. This superior performance of the seed correlates directly with its higher total phenolic content (mg GAE/100 g) and antioxidant capacity (Table 6.), suggesting that the dense concentration of tannins and anthocyanins within the seed matrix facilitates a more effective shielding of the metal surface.

The displacement in corrosion potential (E_{corr}) for all inhibited systems remained within a narrow range (mV) relative to the blank solution. In electrochemical theory, a shift of less than mV indicates that the inhibitor acts as a mixed-type inhibitor, suppressing both the anodic dissolution of iron and the cathodic hydrogen evolution reaction simultaneously (Dehghani et al., 2019). Furthermore, the anodic and cathodic Tafel slopes (β_a and β_c) did not exhibit major changes, implying that the sumac metabolites released from the powder and seed particles inhibit corrosion by geometrically blocking the active sites on the steel surface through adsorption, without altering the fundamental electrochemical reaction mechanism (Verma et al., 2018).

To further elucidate the characteristics of the protective layer, EIS measurements were conducted. The Nyquist plots provide a visual representation of the charge transfer resistance at the metal/electrolyte interface.

Table 7. Effect of sumac powder extract on the potentiodynamic polarization parameters of mild steel in 1 M HCl solution

Inhibitor	C (ppm)	-E _{corr} (mV)	\dot{I}_{corr} (μA)	β_a (mV/dec)	β_c (mV/dec)	Corrosion rate (mpy)	%IE	θ
HCl	-	519	737	112.40	110.3	874.3		
	50	506	568	149.2	147.1	647.5	22.930	0,2293
	100	504	473	137.1	145.6	561.5	35.82	0.3582
	150	506	327	89.3	99	388.8	55.63	0.5563
	200	509	300	76.8	90.3	356.3	59.29	0.5929

*C: inhibitor concentration; E_{corr}: corrosion potential; \dot{I}_{corr} : corrosion current density; β_a and β_c anodic and cathodic Tafel slopes, Corrosion rate: corrosion rate, %IE: inhibition efficiency; θ : surface coverage.

Table 8. Effect of sumac seed extract on the potentiodynamic polarization parameters of mild steel in 1 M HCl solution

Inhibitor	C (ppm)	-E _{corr} (mV)	I _{corr} (μA)	β _a (mV/dec)	β _c (mV/dec)	Corrosion rate (mpy)	%IE	θ
HCl	-	519	737	112.40	110.3	874.3		
	50	506	427	136.3	145.8	506.7	42.060	0.4206
	100	505	359	133.5	144.1	426.9	51.29	0.5129
	150	505	297	127.3	139.7	353.2	59.79	0.5970
	200	500	289	119.5	136	343.5	60.79	0.6079

*C: inhibitor concentration; E_{corr}: corrosion potential; I_{corr}: corrosion current density; β_a and β_c anodic and cathodic Tafel slopes, Corrosion rate: corrosion rate, %IE: inhibition efficiency; θ: surface coverage

The Nyquist plots (Figures 3. and 4.) display single capacitive semicircles, the diameters of which increase significantly with rising concentrations of powder and seed.

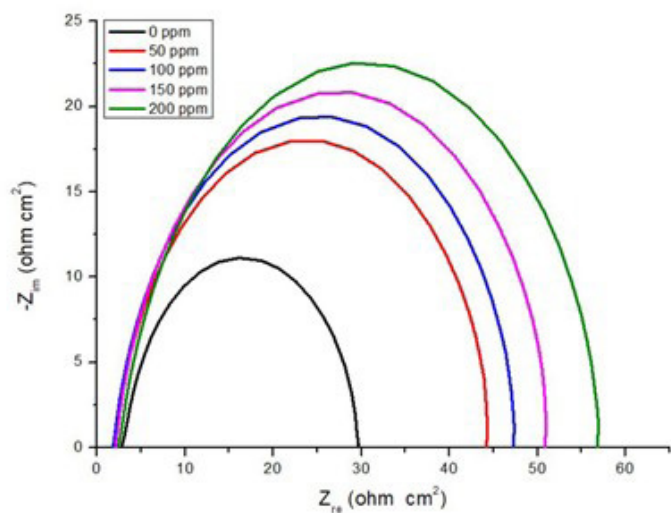


Figure 3. Nyquist plots of carbon steel in 1M HCl solution containing different concentrations of sumac powder extract. Description: The increase in the semicircle diameter with higher concentrations of sumac extract indicates an enhancement in charge transfer resistance (R_t) and an improvement in the corrosion inhibition efficiency.

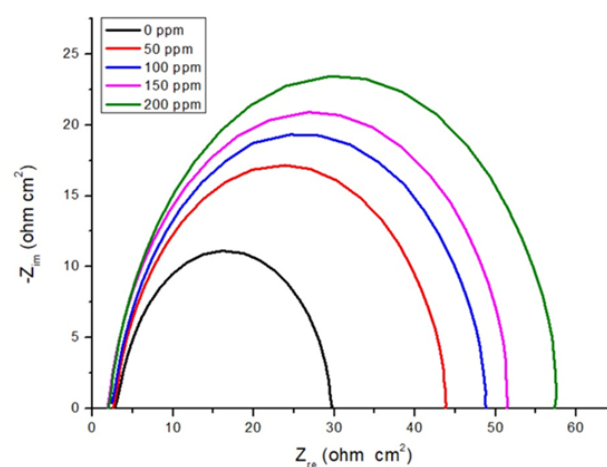


Figure 4. Nyquist plots of carbon steel in 1M HCl solution containing different concentrations of sumac seed extract. Description: The increase in the semicircle diameter with higher concentrations of sumac extract indicates an enhancement in charge transfer resistance (R_t) and an improvement in the corrosion inhibition efficiency.

This expansion reflects a substantial increase in the polarization resistance (R_p), as documented in Tables 9. and 10. The R_p value increased from $25.5 \Omega \cdot \text{cm}^2$ to $52.42 \Omega \cdot \text{cm}^2$ for the seed form at 200 ppm. This increase is attributed to the replacement of water molecules and chloride ions at the metal surface by the bioactive organic molecules released from the sumac matrix, forming a hydrophobic barrier (Fouda et al., 2020).

The “depressed” nature of the semicircles arises from frequency dispersion caused by the surface roughness of the mild steel and the heterogeneous distribution of the adsorbed phenolic film. The higher

R_p and $\% \eta_{EIS}$ values obtained for the seed form compared to the powder form reinforce the conclusion that the seed matrix provides a more robust and compact protective layer. This finding is consistent with the higher mineral and protein stability observed in the seed form (Table 5.), which contributes to the overall structural integrity of the adsorbed inhibitor film (Hussin et al., 2016).

The inhibition mechanism is primarily driven by the adsorption of secondary metabolites from the sumac forms onto the steel surface. The high concentration of hydroxyl groups (-OH) present in the gallic

acid derivatives, tannins, and anthocyanins enables the formation of stable chelates with Fe^{2+} ions. These molecules act as Lewis bases, donating lone pair electrons to the vacant d-orbitals of the iron atoms, thereby establishing a coordinate-type bond. This protective film effectively isolates the metal from the aggressive Cl^- ions, with the seed form demonstrating a more potent effect due to its concentrated phytochemical reservoir.

Table 9. Polarization resistance (R_p) and inhibition efficiency ($\% \eta_{EIS}$) values obtained by the EIS method for the sumac powder inhibitor

	C (ppm)	R_p (ohms)	$\% \eta_{EIS}$
HCl	-	25.5	-
	50	40.14	37.1
	100	43.08	41.39
	150	46.34	45.51
	200	50.88	50.37

*C: inhibitor concentration, R_p : polarization resistance, $\% \eta_{EIS}$: inhibition efficiency obtained from EIS measurements

Table 10. Polarization resistance (R_p) and inhibition efficiency ($\% \eta_{EIS}$) values obtained by the EIS method for the sumac seed inhibitor

	C (ppm)	R_p (ohms)	$\% \eta_{EIS}$
HCl	-	25.5	-
	50	38.86	35.02
	100	43.63	42.13
	150	46.83	46.08
	200	52.42	51.83

C: inhibitor concentration, R_p : polarization resistance, $\% \eta_{EIS}$: inhibition efficiency obtained from EIS measurements.

CONCLUSION

This study provides a comprehensive evaluation of *Rhus coriaria* L. as a multifunctional bioresource, specifically addressing the scientific gap regarding the comparative performance of its powder and seed forms. While sumac has been widely recognized for its biological activities, this research offers an original contribution by demonstrating how biomass morphology and

extraction strategies systematically influence both antioxidant capacity and electrochemical corrosion inhibition.

The investigation into the physicochemical properties and ionic behavior of the extracts reveals that the interaction between the solvent and the plant matrix is a primary determinant of bioactive recovery. The findings emphasize that the seed matrix, often overlooked in industrial processing, acts as a superior reservoir for stabilizing phenolic compounds and proteins

compared to the conventional powder form. This structural preservation within the seed results in enhanced redox-active profiles, which were found to be more resilient during the extraction process.

In the context of material protection, this research establishes that *Rhus coriaria* L. serves as an effective, sustainable, and mixed-type corrosion inhibitor for mild steel in acidic media. The study confirms that the natural metabolites from sumac effectively isolate the metal surface from aggressive ions by forming a stable, adsorbed organic film. A significant outcome of this comparison is the realization that the seed form provides a more robust and compact protective layer than the powder form, likely due to the higher concentration of tannins and anthocyanins that facilitate stable chelation.

Ultimately, this work bridges the gap between food chemistry and materials science by showcasing the dual functionality of sumac. By highlighting the superior performance of the seed form, the study advocates for the valorization of sumac processing byproducts, offering a green alternative to synthetic antioxidants and toxic corrosion inhibitors. Future research should transition toward molecular-level elucidation of the adsorption mechanisms and investigate the long-term durability of these bio-based films in industrial flow systems to fully realize the potential of sumac seeds in advanced bifunctional product design.

CONFLICT OF INTEREST

The authors declare that they have no known competing financial interests or personal relationships that could have appeared to influence the work reported in this paper.

AUTHOR CONTRIBUTIONS

Gülşah Gökce: Conceptualization, Methodology, Investigation, Laboratory Analysis, Writing Original Draft

Bahar Tan Özay: Methodology, Investigation, Laboratory Analysis, Data Curation

Büşra Erdem: Laboratory Analysis, Investigation

Yakup Şirin: Supervision, Writing Review, Editing

Perihan Gürkan: Supervision, Funding Acquisition, Writing Review, Editing

Nurdane Yılmaz: Validation, Writing, Review, Editing.

ACKNOWLEDGEMENT

The authors would like to express their sincere gratitude to all those who contributed to the completion of this research.

Special appreciation is extended to Reşat Gürkan and Semih Gürkan for their valuable support and contributions throughout the study.

REFERENCES

- Abu Reidah, I. M., Ali Shtayeh, M. S., Jamous, R. M., Arráez Roman, D., Segura Carretero, A. (2015). HPLC-DAD-ESI-MS/MS screening of bioactive compounds from *Rhus coriaria* L. (Sumac) fruits. *Food Chemistry*, 181, 284-291.
- Al Amiery, A. A., Isahak, W. N. R. W., Al Amiery, M. H. H. (2023). Recent advances in green corrosion inhibitors derived from plant extracts: A review. *Results in Engineering*, 17, 100930.
- Al Juhaimi, F., Ghafoor, K., Özcan, M. M., Jahurul, M. H. A., Babiker, E. E., Jinap, S. & Zaidul, I. S. M. (2024). Effect of solvent type on phenolics and antioxidant activities of sumac (*Rhus coriaria* L.) fruit. *Journal of Food Measurement and Characterization*, 18(1), 45-56.
- Almuhayawi, M. S. (2022). Comprehensive review of the phytochemical, pharmacological, and therapeutic properties of *Rhus coriaria* L. (Sumac). *Saudi Journal of Biological Sciences*, 29(1), 384-391.
- Al Quraishy, S., Metwally, D. M., El Affi, S. H., Al Abadie, A. S., Abdel Baki, A. S. (2022). *Rhus coriaria* extract attenuates oxidative stress and inflammation. *Journal of King Saud University Science*, 34(4), 102013.
- Alsamri, H., Athamneh, K., Pintus, G., Eid, A. H., Iratni, R. (2021). *Rhus coriaria*: A comprehensive review of its phytochemistry and biological activities. *Molecules*, 26(11), 3125.
- AOAC. (2000). *Official methods of analysis of AOAC International* (17th ed.). Association of Official Analytical Chemists.
- Apak, R., Özyürek, M., Güçlü, K., Çapanoğlu, E. (2016). Antioxidant capacity/activity methods and their applications to fresh and processed foods. *Journal of Agricultural and Food Chemistry*, 64(5), 997-1027.
- Azmir, J., Oliveros Belardo, E., Singh, H. (2013). Techniques for extraction of bioactive compounds from plant materials: A review. *Journal of Food Engineering*, 117(4), 426-436.
- Bedair, M. A., Soliman, S. A., Metwally, A. S., Hegazy, M. A. (2022). Experimental and theoretical studies on the corrosion inhibition of mild steel by *Rhus coriaria* extract in 1M HCl. *Journal of Molecular*

Liquids, 356, 119044.

Benzie, I. F., Strain, J. J. (1996). The ferric reducing ability of plasma (FRAP) as a measure of “antioxidant power”: *The FRAP assay. Analytical Biochemistry*, 239(1), 70-76.

Bursal, E., Köksal, E. (2011). Evaluation of antioxidant capacity and radical scavenging activity of *Rhus coriaria* L. (Sumac). *Food Research International*, 44(9), 2717-2722.

Chemat, F., Abert-Vian, M., Fabiano-Tixier, A. S., Strube, J., Uhlenbrock, L., Gunjevic, V., & Cravotto, G. (2019). Green extraction of natural products. Origins, status, and future challenges. *TrAC Trends in Analytical Chemistry*, 118, 248-263.

Cuendet, M., Hostettmann, K., Potterat, O. (1997). Iridoid glucosides with free radical scavenging properties from *Fagraea blumei*. *Helvetica Chimica Acta*, 80(4), 1144-1152.

Damodaran, S. (2017). Food proteins: An overview. In S. Damodaran & K. L. Parkin (Eds.), *Fennema's Food Chemistry* (5th ed.). CRC Press.

Dehghani, A., Bahlakeh, G., Ramezanzadeh, B. (2019). Detailed macro/micro-scale exploration of the *Rhus coriaria* L. extract as a potent green inhibitor for the mild steel in HCl solution. *Journal of Molecular Liquids*, 279, 15-24.

Doğan, M., Çelik, I. (2012). Determination of some physicochemical and nutritional properties of sumac (*Rhus coriaria* L.) fruits. *Journal of Food Science and Technology*, 49(2), 253-258.

Fouda, A. S., Rashwan, S. M., Abo-Moussa, F. E., & El-Ewady, G. Y. (2020). Natural extract as a green corrosion inhibitor for carbon steel in 1M HCl. *Scientific Reports*, 11, 14923.

Ghafoor, K., Choi, Y. H., Jeon, J. Y., Moon, S. S. (2011). Optimization of ultrasound-assisted extraction of phenolic compounds, antioxidants, and anthocyanins from grape (*Vitis vinifera*) seeds. *Journal of Agricultural and Food Chemistry*, 59(13), 7035-7043.

Gökçe, Ş., Coşkun, Y. (2023). Green corrosion inhibition of steel in acidic media by using sumac extracts. *Journal of Materials Protection*, 12(2), 145-156.

Hussin, M. H., Rahim, A. A., Ibrahim, M. N. M., Brosse, N. (2016).

The capability of ultrafiltered alkaline oil palm fronds lignin as a green corrosion inhibitor of mild steel in 0.5M HCl solution. *Measurement*, 91, 51-60.

Koşar, M., Bozan, B., Temelli, F., Baser, K. H. C. (2006). Antioxidant activity and phenolic composition of sumac (*Rhus coriaria* L.) extracts. *Phytochemical Analysis*, 17(5), 327-334.

Li, Y., Fabiano-Tixier, A. S., Chemat, F. (2021). Comminution as a pre-treatment for extraction of bioactive compounds. *Innovative Food Science & Emerging Technologies*, 68, 102604.

Mert, B., Coşkun, M., Ertürk, S. (2022). Influence of particle size on the extraction of pigments and phenolics from sumac fruits. *Food Chemistry*, 370, 131012.

Mustafa, A., Turner, C. (2011). Pressurized liquid extraction as a green approach in food and herbal plants extraction: A review. *Analytica Chimica Acta*, 703(1), 8-20.

Nawaz, A., Bakhtawar, S., Ahmad, S. (2020). Adsorption mechanism of green corrosion inhibitors in acidic media: A review. *Corrosion Science*, 164, 108342.

Salamat, R., Rahimi, S., Noori, S. (2023). Structural stability and colorimetric properties of sumac anthocyanins. *LWT*, 175, 114482.

Shamsudin, S. (2022). Optimization of extraction parameters for bioactive from *Rhus coriaria*. *Separations*, 9(10), 288.

Slinkard, K., Singleton, V. L. (1977). Total phenol analysis: Automation and comparison with manual methods. *American Journal of Enology and Viticulture*, 28(1), 49-55.

Spigno, G., Tramelli, L., De Faveri, D. M. (2007). Effects of extraction time, temperature and solvent on phenols extraction from grape marc. *Journal of Food Engineering*, 81(1), 200-208.

Uysal, S., Zengin, G. (2021). Bioactive contents of *Rhus coriaria* extracts obtained by different solvents. *Natural Product Research*, 35(12), 2045-2049.

Verma, C., Ebenso, E. E., Bahadur, I., & Quraishi, M. A. (2018). Characterization and corrosion inhibition potential of plant extracts. *Journal of Molecular Liquids*, 249, 18-35.

Wang, L. (2023). Solvent effect on the ionic mobility and extraction yield of botanical compounds. *Journal of Molecular Liquids*, 375, 121345.

Yüksel, E., Kaplan İnce, A. (2023). Redox activity and antioxidant profiles of Turkish sumac genotypes. *Food Bioscience*, 52, 102456.

Zannou, O., Koca, I. (2022). Green extraction of bioactive compounds from sumac (*Rhus coriaria* L.) and their applications. *Journal of Food Process Engineering*, 45(4), e13994.

Cite this article as:

Gökçe G, Tan Özay B, Erdem B, Şirin Y, Gürkan P, Yılmaz N. (2026) Physicochemical, antioxidant and corrosion inhibition properties of *Rhus coriaria* L. extracts obtained using solvents of different polarity. *GIDA* (2026) 51 (2) 327-343 doi: 10.15237/gida.GD25138

Nasıl Atıf Yapılır?:

Gökçe G, Tan Özay B, Erdem B, Şirin Y, Gürkan P, Yılmaz N. (2026) Farklı polaritedeki çözücülerle elde edilen *Rhus coriaria* L. ekstraktlarının fizikokimyasal, antioksidan ve korozyon inhibisyonu özellikleri. *GIDA* (2026) 51 (2) 327-343 doi: 10.15237/gida.GD25138